Cross section of neutrons from the ^{2}H$(n, 2n)$ reaction at $E_n = 15$ MeV

A. V. Voinov,* S. Akhtar, N. Alanazi,† K. Brandenburg, C. R. Brune, T. W. Danley, S. Dhakal,‡ R. Giri,§ T. N. Massey, S. N. Paneru, C. E. Parker,¶ and A. L. Richard**
Department of Physics and Astronomy, Ohio University, Athens, Ohio 45701, USA

C. J. Forrest
Laboratory for Laser Energetics, University of Rochester, 250 East River Road, Rochester, New York 14623-1299, USA

D. Schneider and G. Grim
Lawrence Livermore National Laboratory, 7000 East Avenue, Livermore, California 94551, USA

(Received 28 March 2020; accepted 17 November 2020; published 30 December 2020; corrected 10 March 2021)

The double-differential cross section of the deuteron breakup reaction ^{2}H$(n, 2n)$ has been studied experimentally with a neutron beam energy of 15 MeV. Special attention has been devoted to estimation of background condition and multiple scattering effect in the scattering sample. Experimental data have been compared with models based on phase-space approximation used in the ENDF/B-VIII.0 data library and in the MCNP neutron transport code, as well as with rigorous model based on Faddeev equations used for cross section evaluations in JENDL data library. It was found that experimental data are better reproduced by Faddeev model, however, the model overestimates data in the low-energy region of the neutron spectrum (<4 MeV).

DOI: 10.1103/PhysRevC.102.064005

I. INTRODUCTION

Measurements of the double-differential cross section, $\frac{d\sigma(E,\Theta)}{d\Omega dE}$, of the deuteron (D) ^{2}H breakup D$(n, 2n)$ reaction by 14-MeV neutrons were largely motivated by improving neutron diagnostics of inertial confinement fusion (ICF) experiments at the National Ignition Facility of Lawrence Livermore National Laboratory and the OMEGA laser facility at the University of Rochester. In a laser shot, when temperature and pressure of the deuterium-tritium (DT) fuel in a capsule reaches a certain condition, the D + T fusion reaction[1] starts occurring producing 14-MeV neutrons and α-particles: D+T $\rightarrow n + \alpha + 17$ MeV. Neutrons are of about 14 MeV in energy and interact with D and T components of the cold fuel producing more neutrons from such reactions as D$(n,$ el), D$(n, 2n)$, T$(n,$ el), and T$(n, 2n)$. Resulting neutron yield and energy spectrum contain important information about plasma conditions such as areal density and temperature. Therefore, the neutron diagnostics is used as an important tool in ICF experiments [1].

The breakdown of the total neutron spectrum from DT fuel implosion into components was studied in Ref. [2] where the neutrons from deuteron break up reaction are shown to constitute a substantial fraction in the energy region between 2 and 8 MeV, so that knowledge of an accurate double differential cross section of the deuteron break up reaction is very important for increasing accuracy of the neutron diagnostics in ICF experiments.

Since it is not practical to measure the double differential cross section with high precision at all angles and emitting energies, development of theoretical approaches and benchmarking them against limited experimental data is an essential procedure for advancing our knowledge of the D$(n, 2n)$ cross sections. The deuteron breakup cross sections in the MCNP6 neutron transport code [3] used for neutron diagnostics in ICF experiments are currently based on the ENDF/B-VIII.0 [4] prescription which uses the phase-space distribution law suggested in Ref. [5]. There are more rigorous approaches based on Faddeev theory of few body reactions [6,7]. The Fadeev approach has also been used for D$(n, 2n)$ cross section evaluation in the JENDL-4.0 data library [8].

The current state of available experimental data is shown in Fig. 1. Different experimental data sets were measured by different groups at different angles for outgoing neutrons and at slightly different energies of the neutron beam. Therefore, the figure shows the ratio between experimental cross sections and respective model calculations for which

*voinov@ohio.edu
†Present address: Physics and Astronomy Department, King Saud University, 12371 Riyadh, Saudi Arabia.
‡Present address: Department of Physical Sciences Barry University, Miami Shores, Florida 33161, USA.
§Present address: Holmes Community College, Ridgeland, MS 39157, USA.
¶Present address: Cyclotron Institute, Texas A&M University, College Station, Texas 77843, USA.
**Present address: National Superconducting Cyclotron Laboratory, Michigan State University, East Lansing, MI 48824, USA

[1]Throughout the text, 'D' and 'T' denote '^{2}H' and '^{3}H', respectively. And we use the reaction abbreviation '$(n,$ el)' to denote inelastic neutron scattering, '(n, n_{el})'.

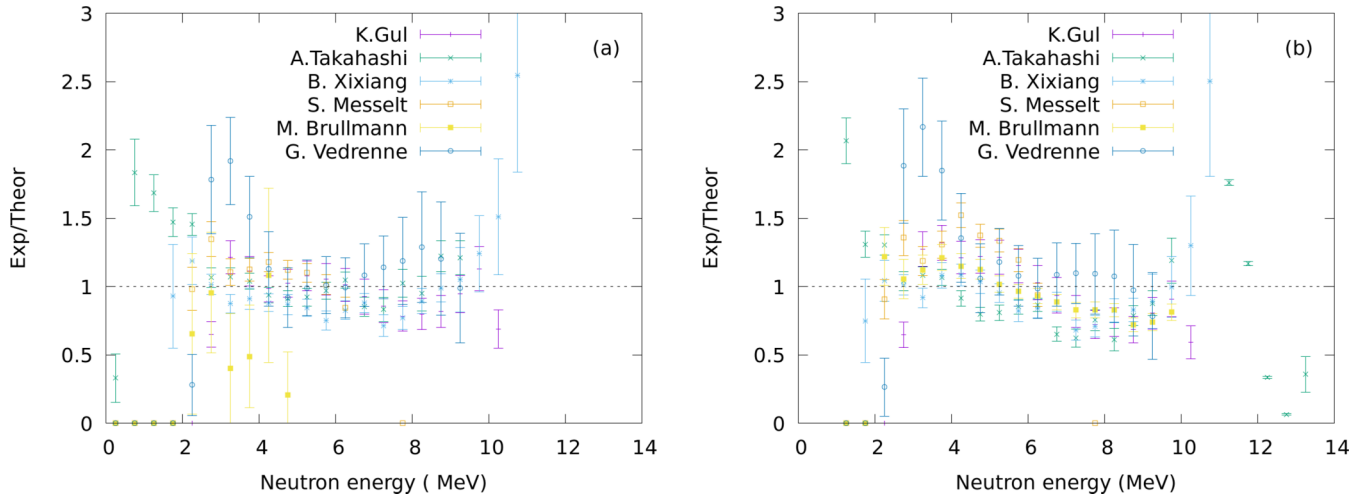

FIG. 1. Ratios of experimental data points available in EXFOR [9] data base and JENDL (a) and MCNP (ENDF/B-VIII.0) (b) model calculations. Data points are from the following references: Gul [10], Takahashi [11], Xixiang [12], Messelt [13], Brullmann [14,15], Vedrenne [16]. Data correspond to measured angles between 25° and 40° in laboratory system.

both the JENDL model based on Faddeev approach and the ENDF/B-VIII.0 phase-space distribution model were used. All data points shown in Fig. 1 correspond to measured angles between 25° and 40°. One can see that the spread of experimental data points is large, especially in lower energy regions. This motivates further research on this subject. In this paper, experimental measurements of neutron spectra emitted from the D$(n, 2n)$ reaction with 15-MeV neutrons has been conducted at the Edwards Accelerator Laboratory with the Swinger neutron time of flight facility. It has been accompanied by rigorous neutron transport Mote Carlo simulations aimed at properly taking into account background conditions and multiple neutron scattering in scattering samples.

II. EXPERIMENTAL SETUP

The neutron facility at the Edwards Laboratory includes a Swinger magnet and a 30 m well shielded time of flight underground tunnel. The Swinger magnet allows rotating the beam line around the scattering sample position thereby allowing measurements of the angular distribution of outgoing neutrons. The tunnel is shielded from the target area by about 1.5 meter thick high density concrete wall with a collimator hole in it (see Fig. 2). A collimator consisted of nylon cylindrical blocks properly sized to match the size of a cone determined by sizes of both scattering sample and detector as well as by the distance between them.

A. Neutron source

For the neutron production we used the D-T reaction with a tritiated titanium target and 0.5 MeV deuteron pulsed beam from the tandem accelerator of the Edwards Accelerator Laboratory. 0.5 MeV deuterons on a stopping tritium target produced neutrons with an average energy of 15.1 MeV at 0° in the laboratory frame. The calculated neutron spectrum is shown in Fig. 3. In the experiment, the tritium target was mounted on a steel plate attached to the bottom of aluminum cylindrical chamber (see Fig. 2 for exact geometry). Therefore, the neutron spectrum is expected to be more complicated due to contribution of neutrons scattered from surrounding construction materials. Real spectra will be discussed in Sec. III.

B. Scattering samples

We used D_2O (heavy water) scattering sample to measure breakup neutrons from the D$(n, 2n)$ reaction. The H_2O (normal water) scattering sample was used to study contribution due to scattering of neutrons on oxygen. Normal and heavy water were enclosed in plastic containers having shapes of a truncated cone. The weight of the empty container was 3.2 g and weights of normal and heavy water in them were 59 and 65.5 g, respectively. The weights were adjusted to keep approximately the same number of atoms in both samples, however, since water evaporates in time, the actual weight was determined before each measurement and corresponding corrections were used in data analysis.

C. Neutron detector

One 5-inch diameter 2-inch thick detector filled with a NE213 liquid scintillator was setup in the tunnel at 8 m distance from the scattering sample. Pulse-shape discrimination was used to separate γs from neutrons. The low energy threshold for neutrons was about 1 MeV.

D. Method

The neutron spectrum produced from the deuteron break up reaction occurring in heavy water sample is expected to be distorted by the following parasitic effects: (a) elastic and inelastic scattering of neutrons on oxygen contained in heavy water sample, (b) multiple scattering effect on both oxygen and deuterons contained in the sample, (c) multiple scattering of neutrons by construction materials surrounding the neutron production tritium target including but not limited to, tritium target chamber, concrete walls in experimental area, large

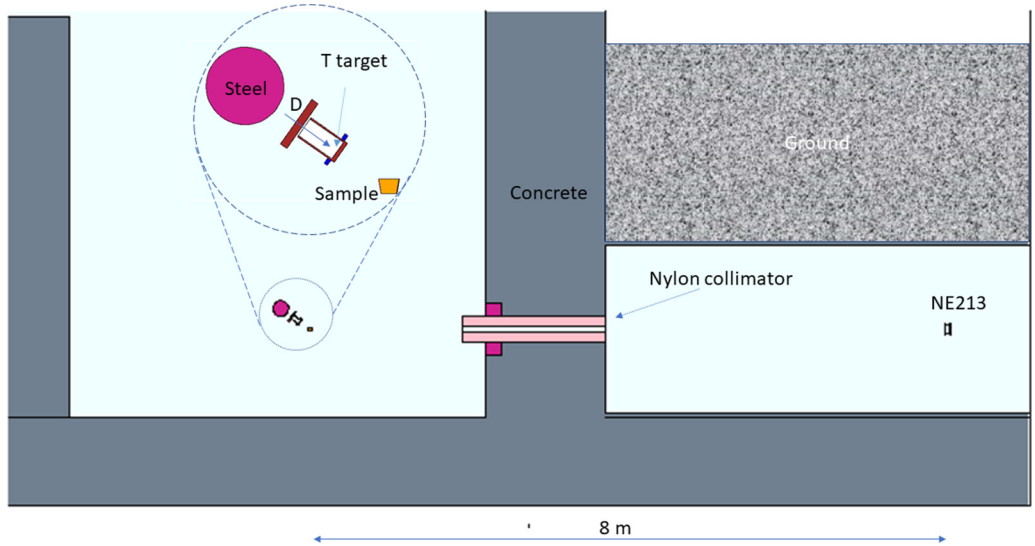

FIG. 2. Layout of the experimental geometry for the D(n, $2n$) experiment at the Edwards Accelerator Laboratory. D stands for the ^{2}H nucleus.

amount of construction steel of the swinger magnet, air in the experimental hall, neutron nylon collimator in the tunnel shielding wall. Therefore, full Monte Carlo neutron transport simulations were performed to properly take into account those parasitic effects. That was considered to be an important part of data analysis. It would also give us an indispensable input for possible improvement of experimental conditions to plan future experiments.

III. NEUTRON TRANSPORT MONTE CARLO SIMULATION

The Monte Carlo N-Particle (MCNP) computer code MCNP6 [3] was used for neutron transport simulations. The experimental geometry used as an input for simulations took into account only those construction elements which were estimated to be the main contributors of scattered neutrons to the measured neutron spectra. To determine important elements, multiple test simulations have been performed.

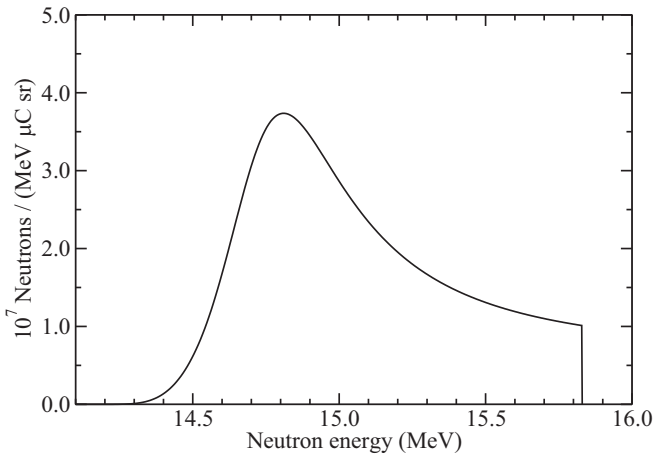

FIG. 3. Calculated neutron spectrum produced by 0.5 MeV deuterons impinged on a stopping tritium target. The spectrum corresponds to 0° of outgoing neutrons.

Figure 2 shows the MCNP input geometry for the neutron source chamber, scattering sample, and experimental area. The neutron field of the source in the MCNP input was described by the energy-angular distribution of outgoing neutrons which is determined by both the T(d, n) reaction kinematic and cross sections in the 0–500 keV deuteron energy range in a stopping tritium target. The angular distribution of outgoing neutrons was assumed to be isotropic which is consistent with experimental data available in literature [9].

The neutron detection efficiency has been studied in the Edwards Accelerator with both a californium neutron source and the ^{27}Al(d, n) reaction on a thick stopping aluminum target [17]. The specific detector used in these measurements has been extensively studied and results are presented in Ref. [18]. Results show that in the neutron energy range up to at least 10 MeV, the NE213 detector efficiencies are well reproduced by Monte Carlo calculations with precision less than 5%. Therefore, the efficiencies for MCNP input were calculated in the range of 1–15 MeV with the SCINFUL Monte Carlo program [19]. The low-energy threshold in calculations has been adjusted to match the experimental one.

A. Multiple scattering effects in scattering samples

It is common for neutron scattering experiments that scattering sample has a large quantity of material. Therefore, it is a concern that neutrons can interact multiple times in the sample before they escape it. This results in distortion of the measured spectrum. The specific processes contributing to it are following.

(i) Attenuation of neutrons passing through the sample and air. This is due to mostly elastic collisions with protons (in a normal water sample), deuterons (in a heavy water sample), with oxygen in both samples, and with oxygen and nitrogen in air. Different

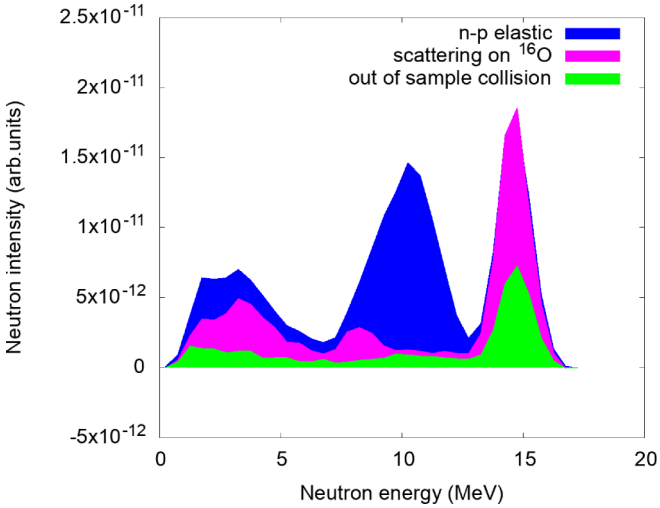

FIG. 4. MCNP simulated neutron spectrum for 35° of outgoing neutrons from H_2O scattering sample. The spectrum is broken down into components corresponding to interaction of neutrons with different materials in and out of scattering sample.

attenuation for neutrons with different energies might affect the measured shape of a deuteron break-up spectrum.

(ii) Multiple elastic and inelastic scattering can result in downgrading neutron energies in the sample, and some of the downgraded neutrons can escape the sample in the direction of a neutron detector. Such neutrons are expected to contribute to the low-energy part of the measured spectra. In our case, elastic neutron scattering on protons, deuterons and oxygen contained in the samples produces strong mono energetic peaks in spectra. Multiple scattering effect results in downgrading some fraction of those neutrons towards the low energy region of the spectra. This is illustrated by Fig. 4 where MCNP simulated spectrum from a normal water sample has been broken down into components corresponding to interaction of neutrons with elements contained in and out of the sample (hydrogen in the sample and oxygen in the sample and air). One can see the presence of the low energy tail due to multiple elastic scattering events on hydrogen.

Because scattering cross sections on protons are different from those on deuterons, subtracting the spectrum of normal water sample from that of heavy water sample might leave nonzero remaining contribution to the difference spectrum. Instead of estimating each effect listed above individually, we estimated the combined effect on the spectrum obtained from the difference between the neutron spectrum from heavy water sample and the spectrum from normal water sample. It has been estimated by executing the MCNP code for our experimental geometry. In order to speed up calculations, all neutrons were directed on the scattering sample using mono-directional neutron source in an MCNP input file. This reduced background from neutrons scattered on construction materials and air which otherwise contributed about 10% as is seen from Fig. 4. However, if we assume that this background is same for both H_2O and D_2O samples, it is expected to be canceled out when implementing the subtraction procedure.

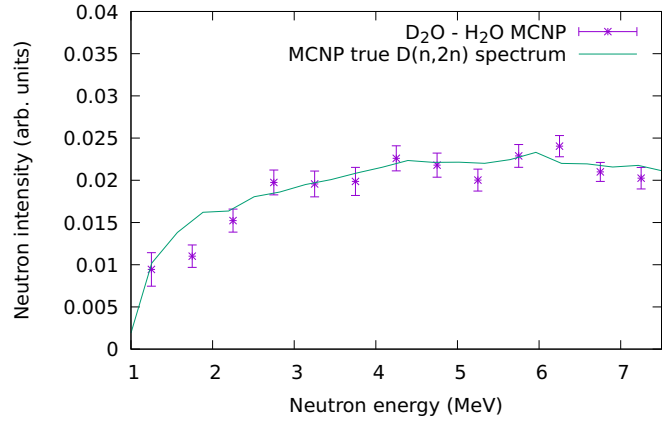

FIG. 5. The $D_2O - H_2O$ difference spectrum obtained from MCNP simulations with real experimental conditions compared to the true model neutron spectrum from D$(n, 2n)$ used in MCNP code. D stands for the deuteron ^{2}H nucleus.

Since, in the next section, we will be focusing on analysis of experimental spectra measured at 35° angle, test MCNP simulations have been also performed for 35° for both heavy and normal water samples. The difference $D_2O - H_2O$ spectrum is shown in Fig. 5 in comparison with the spectrum obtained from separate MCNP run for the same angle performed with an unreal 10 times lower density deuterium scattering sample and no air between the sample and detector so that multiple scattering effects were neglected. The neutron spectrum obtained from the latter simulations is assumed to be "true" neutron spectrum produced by MCNP model which is free from any contaminations due to multiple scattering effects. The difference spectrum was corrected on absorptions in both scattering sample and in air which were determined with a separate MCNP run. One can see that the shape of the difference spectrum obtained from MCNP calculations using real experimental conditions is in good agreement within less than 10% with the shape of the 'true' D$(n, 2n)$ neutron spectrum produced from MCNP when all multiple scattering and absorption effects were removed. Absolute scale for both spectra is arbitrary in this figure. Spectra were scaled to match absolute values just to show the comparison of shapes of the neutron energy distribution. The absolute normalization will be discussed in the next section.

IV. EXPERIMENT

Measurements of neutron spectra from heavy water and normal water scattering samples have been conducted at different angles of outgoing neutrons. At this stage of the experimental measurements the goal was to test (at least roughly) MCNP simulations to confirm that the MCNP input describing the experimental setup makes sense. Therefore, these runs were not intended to acquire good counting statistics. Figure 6 presents experimental and calculated neutron spectra measured without the scattering sample in place at

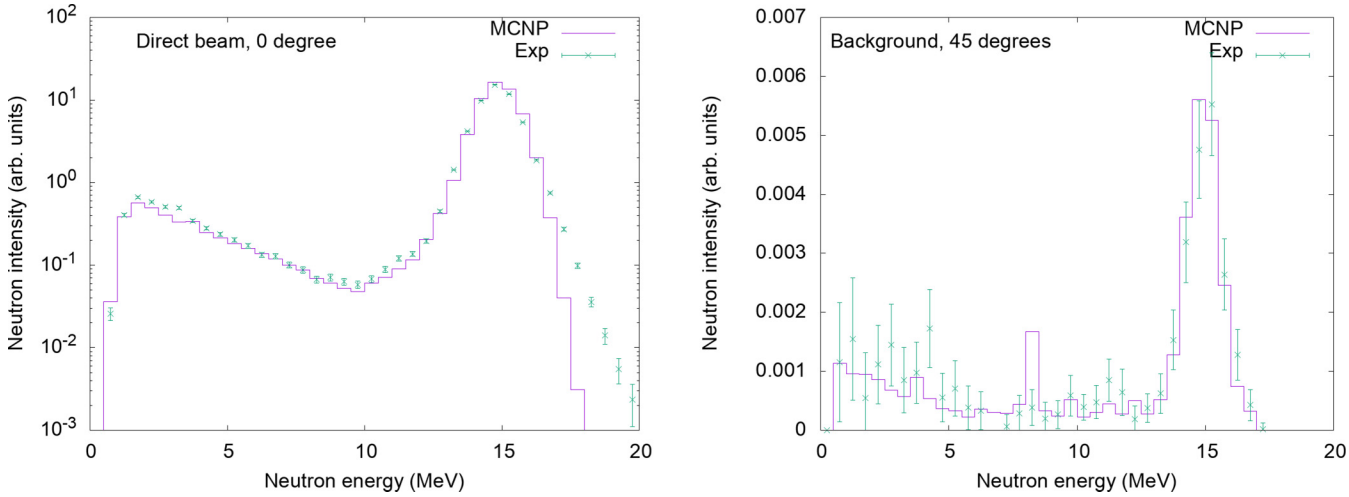

FIG. 6. Experimental and MCNP simulated neutron spectra at 0° and 45° in the laboratory frame with no sample in place.

0° (corresponding to direct measurements of neutrons emitted by the neutron production tritium target), and 45° angles. It shows a good agreement between data points and MCNP calculations within error bars. Discrepancy in high energy tail of the 15-MeV peak at 0° is presumably due to poor reproduction of the high energy tail of the pulsed beam time structure for this specific run. It does not seem to be a problem for other spectra presented here. The 15 MeV peak in the neutron

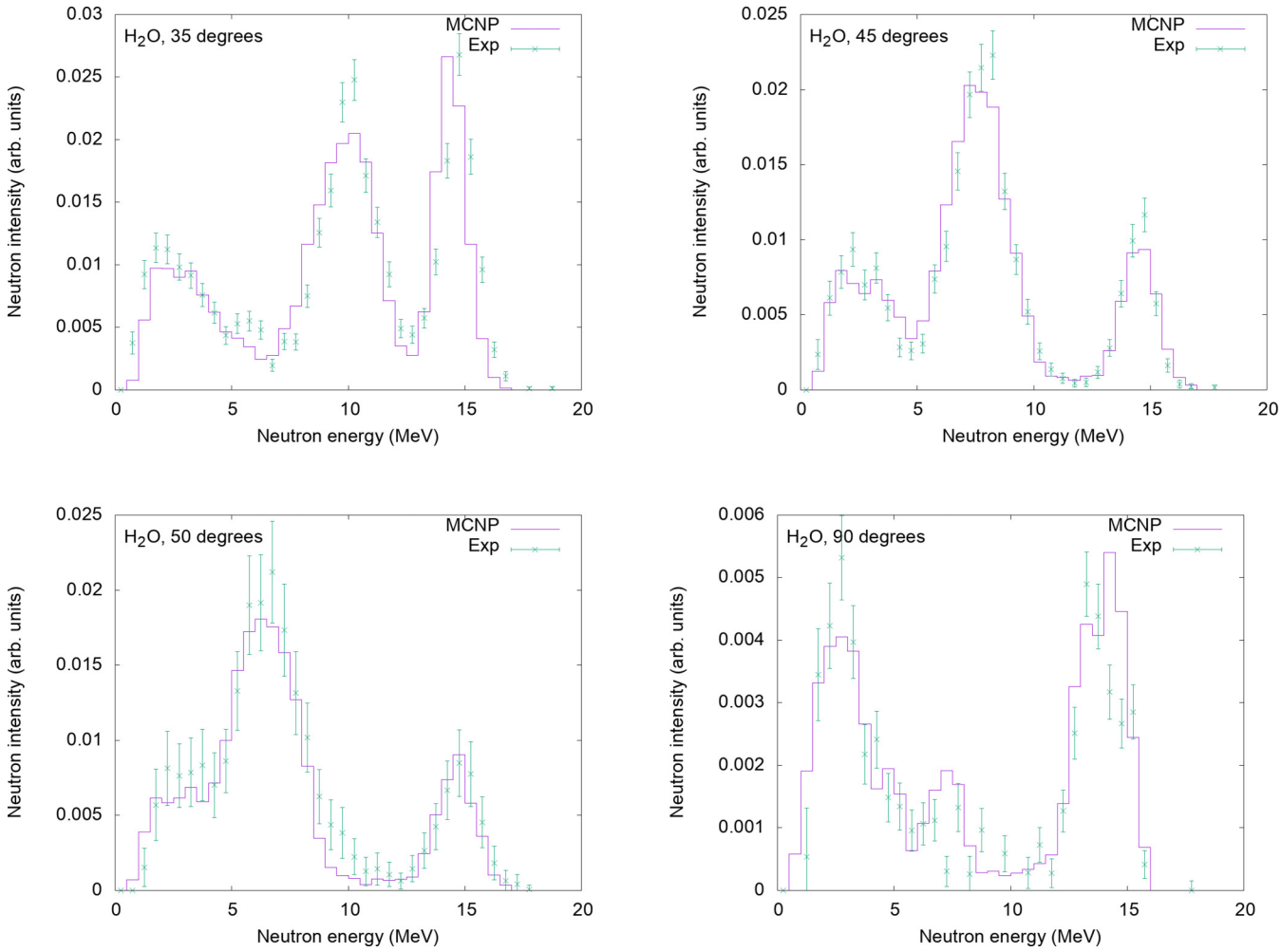

FIG. 7. Experimental and MCNP simulated neutron spectra at 35°, 45°, 50°, and 90° in the laboratory frame with H_2O sample.

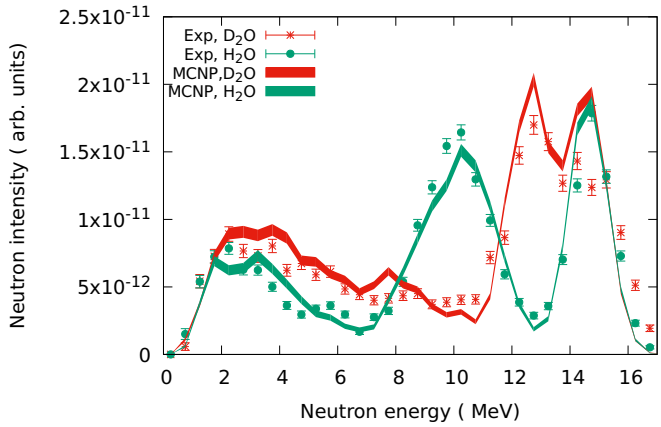

FIG. 8. Experimental and MCNP simulated neutron spectra at 35° in the laboratory frame. D stands for the ^{2}H nucleus.

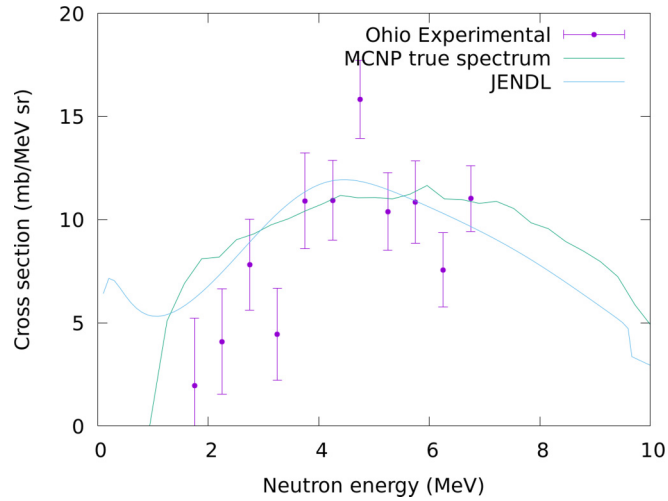

FIG. 9. Experimental cross sections for the D$(n, 2n)$ reaction obtained as a difference of neutron spectra measured with deuterated water D_2O and normal water H_2O scattering samples for 35° angle in the laboratory system.

spectrum measured at 45° is caused by elastic scattering of 15 MeV neutrons on oxygen and nitrogen in the air at forward angles. The low energy tails on both panels in the figure are caused by multiple scattering events in air and construction materials. Neutron intensities are presented in arbitrary units. The scaling factor for all MCNP simulated neutron spectra was determined from the ratio of experimental and calculated spectra for the 0° angle. When comparing simulated and experimental spectra for different angles, the same scaling factor was applied. All experimental spectra have been normalized based on integrated beam charge accumulated during each run. Experimental and MCNP simulated neutron spectra measured with the H_2O scattering sample at different angles, which are shown in Fig. 7. Reasonable agreement between experiment and simulations was obtained.

V. ABSOLUTE CROSS SECTIONS OF D$(n, 2n)$

The absolute cross sections of the deuteron break up reaction D$(n, 2n)$ were determined relative to the elastic H(n, el) cross section which is well known with high precision [20]. Based on conclusions from Sec. III A, the neutron spectrum from the deuteron break-up reaction can be obtained by subtracting the neutron spectrum measured with a normal water sample from that measured with a heavy water sample. For further analysis we have chosen the neutron spectra measured at 35° angle since the elastic scattering peak in normal water sample has a high enough energy such that it has smaller interference with the energy region of interest. Experimental spectrum was accumulated for about 11 hours for the heavy water sample and for about 22 hours for the normal water sample. Spectra from both samples and corresponding MCNP calculations are presented in Fig. 8. Before the subtraction procedure was implemented, experimental neutron spectra were scaled with a normalization coefficient determined as a ratio of areas under the elastic scattering peaks in H_2O spectra. The second renormalization coefficient was used to convert units in the difference $D_2O - H_2O$ spectrum to the units of the absolute cross section. This normalization coefficient was calculated as a ratio of elastics scattering cross section on protons at 35° and the area of the elastic scattering peak in the H_2O MCNP simulated spectrum. A value of 163 mb for the elastic scattering H(n, el) cross section for the 15 MeV neutrons and 35 scattering angle has been obtained from ENDF/B-VIII.0 library. In order to determine the net area of elastic scattering peak in the MCNP H_2O spectrum, the area under the peak should be properly subtracted (see Fig. 8). This background is caused by inelastic and multiple scattering events mainly from neutrons scattered on oxygen in the sample, oxygen and nitrogen in the air and on the nylon collimator containing hydrogen and carbon. All these contributions have been separately calculated with full MCNP simulation and shown in Fig. 4. For absolute normalization, the net neutron spectrum (which is free from contributions of neutrons scattered on other materials) corresponding to elastic scattering on hydrogen in the sample has been extracted and the area under the elastic scattering peak was determined.

The experimental cross sections were then obtained and corrected on attenuation in the sample and air. They are shown in Fig. 9 along with calculations from JENDL and MCNP (ENDF/B-VIII.1) models. The ratios of experimental and model cross sections are shown in Fig. 10. One can see that model calculations tend to overestimate data points in the energy region below 4 MeV.

VI. COMPARISON WITH DATA OBTAINED FROM OMEGA LASER FACILITY

It is interesting to compare our results with results obtained in the recent paper by Forrest *et al.* [21]. Authors measured deuteron break cross sections with 14 MeV neutrons produced by fusion reaction with laser beams at OMEGA laser facility [22]. Neutrons from D$(n, 2n)$ break up have been measured at the 0°–7° average angle with C_6D_6 and D_2O scattering samples. Data points in the low energy region were shown to be overestimated by the model which uses exact solution of Faddeev equations including $3N$ forces. We found that the

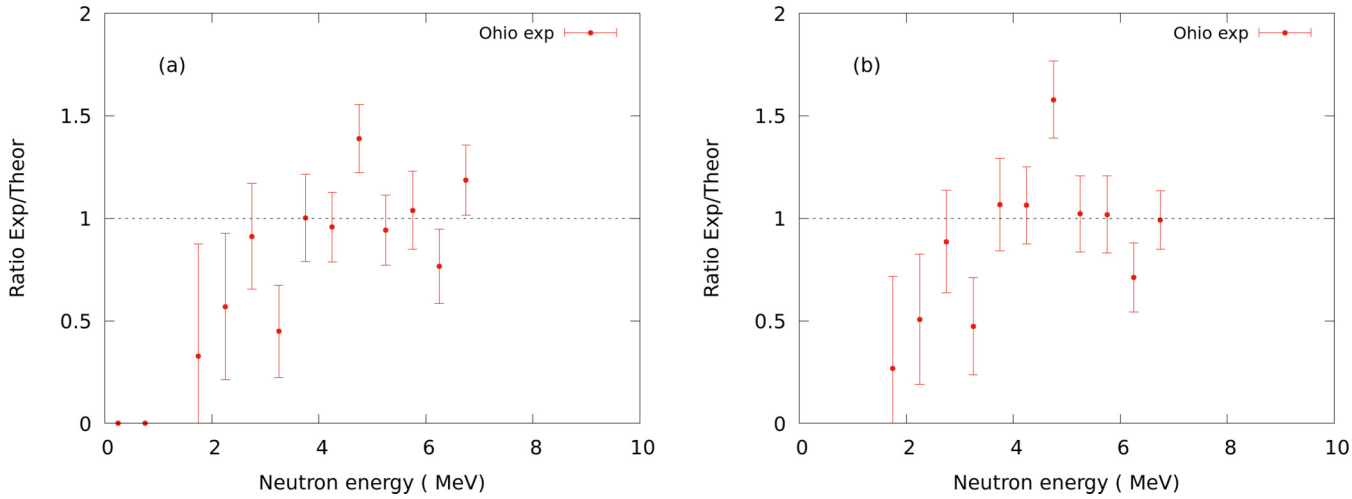

FIG. 10. Ratio of experimental and model cross sections. (a) is for the JENDL model and (b) is for the MCNP (ENDF/B-VIII.0) model.

JENDL model provides very similar results. Here we calculated the ratio of experimental cross sections from Ref. [21] to those calculated with JENDL and MCNP (ENDF/B-VIII.0) models (see Fig. 11). One can see that it has the similar tendency to what was obtained from our experiment (presented in Fig. 10), i.e., experimental cross sections are lower than that predicted by models in the low energy region. Therefore one can point out that our data show consistency with OMEGA data. This can be seen as confirmation that results obtained from both experiments exhibit the same physical feature.

VII. DISCUSSION AND CONCLUSION

Neutron spectra from normal water and heavy water samples measured at 35° angle with the Swinger neutron facility of the Edwards Accelerator Laboratory have been analyzed and cross sections have been deduced according to the method described above. We showed that despite of the presence of multiple scattering events in scattering samples (see Fig. 4), the spectrum of neutrons and corresponding double differential cross sections can be deduced from subtraction of neutron spectrum measured with normal water sample from one measured with heavy water sample. Systematical uncertainties in the shape of the difference spectrum were estimated to be less than 10% for our experimental conditions.

As is seen from Fig. 10, experimental cross sections obtained from our measurements are in agreement within error bars with both JENDL and MCNP (ENDF/B-VIII.0) model calculations in the energy region between 4 and 7 MeV. For neutrons below 4 MeV experimental points tend to be lower than model predictions. Because error bars are large, this observation is considered to be preliminary and needs to be confirmed from future experiments. However, the fact that this observation is consistent with a similar observation from the OMEGA experiment of Ref. [21], makes this conclusion more reliable. This could be interesting from point of view of developing few-body theoretical models. From the experimental point of view, the low energy region is prone to

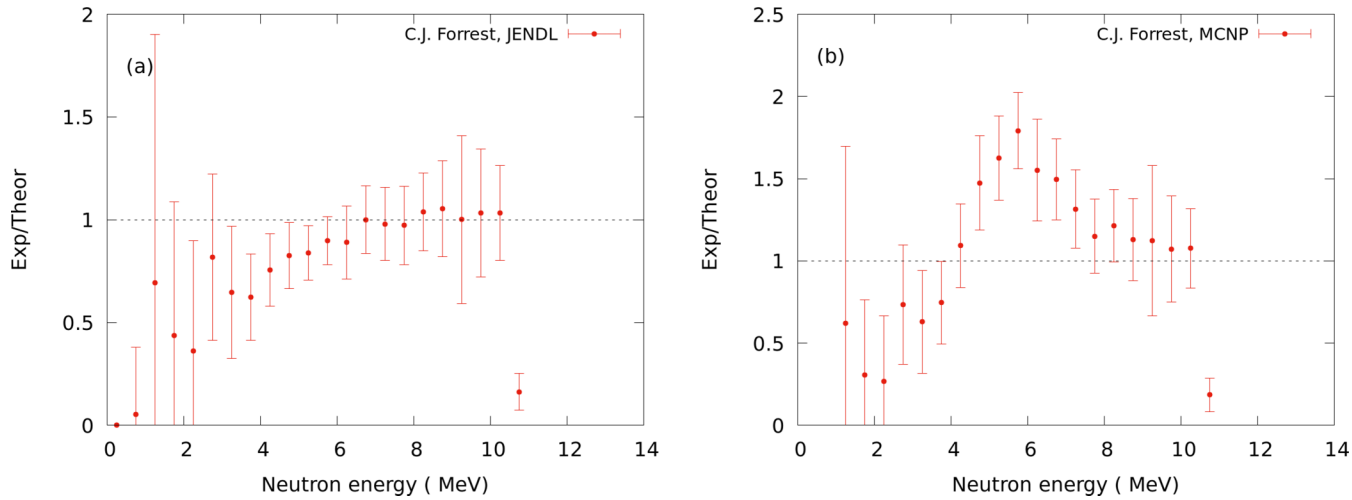

FIG. 11. Ratio of experimental and model cross sections. Experimental cross sections are from Ref. [21]. (a) is for the JENDL model and (b) is for the MCNP (ENDF/B-VIII.0) model.

accumulating background neutrons scattered from everywhere, since all scattered neutrons degrade in energy. Therefore, reducing scattered neutrons and accounting for them correctly is an important problem for experimental design and data analysis. That might be one of the reasons for the difference between data sets obtained from different experiments presented in Fig. 1. MCNP simulations of the full experimental set up are necessary for understanding and taking into account all components of the measured spectra. This approach might distinguish the data analysis presented in this report from analysis of analogous experiments conducted earlier by different groups.

Statistical error bars on experimental points obtained in our measurements are on the order of 20–30%. This is result of 11 hours statistics accumulation for the heavy water sample and of about 22 h for the normal water sample. It is obvious that the statistical errors can be reduced by increasing accumulation time during experiments that would be possibility for future experimental campaigns. Among other possible improvements of the experimental setup one can mention the different shape design of the scattering sample in order to reduce the angular spread of incoming neutron beam. About 13° angular spread in current experiments resulted in a wide [3 MeV for H(n, el)] elastic scattering peak in neutron spectra which overlaps with the region of interest of break up neutrons. There is also possibility to reduce scattered low energy neutrons from the back wall of the experimental hall as seen by detector. They were found to be a non-negligible source of contributions to the measured neutron spectra.

In conclusion one can state that the models which use a rigorous solution of Faddeev equations reproduce data points more accurately compared to the model based on phase space approximation used in ENDF evaluations and which is currently embedded in MCNP neutron transport code. This is in agreement with results of earlier works, such as Ref. [11]. It was also found that despite of relatively large statistical uncertainties of experimental cross sections obtained in this experiment, cross sections in the low energy region tend to be smaller compared to available models. This is in agreement with a recent work of Ref. [21]. This finding might motivate further studies of this phenomenon.

For practical applications including neutron diagnostics in ICF experiments, this means that replacing the phase-space approximation model for the deuteron break-up reaction by the model based on Faddeev equations in MCNP neutron transport code should reduce uncertainties in analysis of neutron yield and its energy and spacial distribution.

ACKNOWLEDGMENTS

Authors acknowledge financial support from U.S. Department of Energy, Grants No. DE-NA0002905, No. DE-FG02-88ER40387, and Lawrence Livermore National Laboratory subcontract, No. B610277.

[1] R. Hatarik, D. B. Sayre, J. A. Caggiano, T. Phillips, M. J. Eckart, E. J. Bond, C. Cerjan, G. P. Grim, E. P. Hartouni, J. P. Knauer, J. M. Mcnaney, and D. H. Munro, J. Appl. Phys. **118**, 184502 (2015).

[2] C. J. Forrest, Measurements of the fuel distribution in cryogenic D-T direct-drive implosions, Ph.D. thesis, University of Rochester, Rochester, NY, 2015.

[3] T. Goorley, M. James, T. Booth, F. Brown, J. Bull, L. J. Cox, J. Durkee, J. Elson, M. Fensin, R. A. Forster, J. Hendricks, H. G. Hughes, R. Johns, B. Kiedrowski, R. Martz, S. Mashnik, G. McKinney, D. Pelowitz, R. Prael, J. Sweezy, L. Waters, T. Wilcox, and T. Zukaitis, Nuclear Technology **180**, 298 (2012).

[4] D. Brown, M. Chadwick, R. Capote, A. Kahler, A. Trkov, M. Herman, A. Sonzogni, Y. Danon, A. Carlson, M. Dunn, D. Smith, G. Hale, G. Arbanas, R. Arcilla, C. Bates, B. Beck, B. Becker, F. Brown, R. Casperson, J. Conlin, D. Cullen, M.-A. Descalle, R. Firestone, T. Gaines, K. Guber, A. Hawari, J. Holmes, T. Johnson, T. Kawano, B. Kiedrowski, A. Koning, S. Kopecky, L. Leal, J. Lestone, C. Lubitz, J. M. Damián, C. Mattoon, E. McCutchan, S. Mughabghab, P. Navratil, D. Neudecker, G. Nobre, G. Noguere, M. Paris, M. Pigni, A. Plompen, B. Pritychenko, V. Pronyaev, D. Roubtsov, D. Rochman, P. Romano, P. Schillebeeckx, S. Simakov, M. Sin, I. Sirakov, B. Sleaford, V. Sobes, E. Soukhovitskii, I. Stetcu, P. Talou, I. Thompson, S. van der Marck, L. Welser-Sherrill, D. Wiarda, M. White, J. Wormald, R. Wright, M. Zerkle, G. Žerovnik, and Y. Zhu, Nucl. Data Sheets **148**, 1 (2018), Special Issue on Nuclear Reaction Data.

[5] P. G. Young, Los Alamos National Laboratory Report No. LA-9468-PR (1984).

[6] A. Deltuva, A. C. Fonseca, and P. U. Sauer, Phys. Rev. Lett. **95**, 092301 (2005).

[7] W. Ebenhöh, Nucl. Phys. A **191**, 97 (1972).

[8] K. Shibata, O. Iwamoto, T. Nakagawa, N. Iwamoto, A. Ichihara, S. Kunieda, S. Chiba, K. Furutaka, N. Otuka, T. Ohsawa, T. Murata, H. Matsunobu, A. Zukeran, S. Kamada, and J. Katakura, J. Nucl. Sci. Technol. **48**, 1 (2011).

[9] V. Zerkin and B. Pritychenko, Nucl. Instrum. Methods Phys. Res. A **888**, 31 (2018).

[10] K. Gul, A. Waheed, M. Ahmad, M. Saleem, and N. A. Khan, J. Phys. G **5**, 1107 (1979).

[11] A. Takahashi, J. Yamamoto, K. Oshima, M. Ueda, M. Fukazawa, Y. Yanagi, J. Miyaguchi, and K. Sumita, J. Nucl. Sci. Technol. **21**, 577 (1984).

[12] B. Xixiang, W. Shenlin, S. Daze, L. Anli, C. Guanren, H. Tangzi, and S. Fengxian, Chinese J. Nuclear Physics (Beijing) **2**, 327 (1980).

[13] S. Messelt, Nucl. Phys. **48**, 512 (1963).

[14] M. Brüllmann, H. Jung, D. Meier, and P. Marmier, Phys. Lett. B **25**, 269 (1967).

[15] M. Brüllmann, H. Jung, D. Meier, and P. Marmier, Nucl. Phys. A **117**, 419 (1968).

[16] G. Vedrenne, D. Blanc, and F. Cambou, J. Phys. (France) **24**, 801 (1963).

[17] T. N. Massey, S. Al-Quraishi, C. E. Brient, J. F. Guillemette, S. M. Grimes, D. Jacobs, J. E. O'Donnell, J. Oldendick, and R. Wheeler, Nucl. Sci. Eng. **129**, 175 (1998).

[18] N. Kornilov, Verification of the ^{252}Cf standard in the energy range 2–20 MeV, (2015), iAEA report, INDC(USA)-108.

[19] J. K. Dickens, SCINFUL: A Monte Carlo based computer program to determine a scintillator full energy response to

neutron detection for E_n between 0.1 and 80 MeV: Program development and comparisons of program predictions with experimental data (1988), ORNL-6463.

[20] M. B. Chadwick, M. Herman, P. Obložinský *et al.*, Nucl. Data Sheets **112**, 2887 (2011).

[21] C. J. Forrest, A. Deltuva, W. U. Schröder, A. V. Voinov, J. P. Knauer, E. M. Campbell, G. W. Collins, V. Y. Glebov, O. M. Mannion, Z. L. Mohamed, P. B. Radha, S. P. Regan, T. C. Sangster, and C. Stoeckl, Phys. Rev. C **100**, 034001 (2019).

[22] C. Forrest, J. Knauer, W. Schroeder, V. Glebov, P. Radha, S. Regan, T. Sangster, M. Sickles, C. Stoeckl, and J. Szczepanski, Nucl. Instrum. Methods Phys. Res. A **888**, 169 (2018).

Correction: The previously published Figure 9 contained an error in the scale on the ordinate and has been replaced.